

# Crystallization and Solidification Studies in Calcia–Alumina Fibres Formed Via Inviscid Melt Spinning (IMS)

Brian S. Mitchell

Department of Chemical Engineering, Tulane University, New Orleans, LA 70118, USA

(Received 21 May 1996; accepted 10 September 1996)

**Abstract:** Differential thermal analysis (DTA) is used to study solidification phenomena in 46.5 wt% CaO–53.5 wt%  $\text{Al}_2\text{O}_3$  (m.p. = 1392°C) fibres formed via inviscid melt spinning (IMS). After an initial heating cycle at  $20^\circ\text{C min}^{-1}$  in nitrogen to 1600°C showing crystallization of the amorphous fibres, cooling curves indicate a solidification exotherm at 1403°C, followed by two small exotherms, believed to be solidification of sub-solidus liquid. Subsequent heating cycles show no crystallization transformations, indicating near complete crystallization upon cooling between heating cycles. XRD results obtained after a final cooling step show two anhydrous calcium aluminate phases are present:  $\text{CaAl}_2\text{O}_4$  and  $\text{Ca}_3\text{Al}_2\text{O}_6$ . © 1997 Elsevier Science Limited and Techna S.r.l.

## 1 INTRODUCTION

Careful control of crystallite nucleation and growth in amorphous calcium oxide/aluminium oxide fibres is important for a number of potential applications that have been identified for these fibres. In particular, their infrared transmission capabilities and mechanical properties depend on such parameters as crystallite size, bulk vs surface crystallization and the specific phases present after crystallization. The purpose of this investigation is to build upon the limited body of knowledge currently available on crystallization and metastable phase formation in amorphous calcium oxide/aluminium oxide fibres through differential thermal analysis (DTA), specifically cooling curves, and X-ray diffraction (XRD) studies.

The calcium oxide/aluminium oxide fibres under consideration in this discussion (often called calcia–alumina, or calcium aluminate fibres) are those formed via the inviscid melt spinning (IMS) process. IMS is a melt-processing technique in which fibres are formed directly from the melt by stream stabilization in a reactive gas atmosphere, in this case, propane.<sup>1</sup> At a given quench rate, calcium oxide–aluminium oxide fibres formed in this man-

ner can be either X-ray amorphous or crystalline, depending on alumina composition. This relationship between crystallinity and composition is not yet entirely clear, but melt viscosity seems to play an important role, at least over the range of compositions studied to date ( $> 50$  wt%  $\text{Al}_2\text{O}_3$ ). Melt viscosity decreases from 10 to less than 0.1 Pa·s between 50 and 80 wt%  $\text{Al}_2\text{O}_3$ . Crystal growth kinetics depend heavily on viscosity, so substantial decreases in viscosity, whether caused by temperature, composition, or a combination of both, greatly enhance crystal growth. Solidification rates also play a major role in determining the structure of IMS fibres. The formation of amorphous calcia–alumina fibres can be attributed partly to the high solidification rates inherent in the IMS process. Quench rates have been estimated at  $10^3$ – $10^4$  K s<sup>−1</sup> for IMS.<sup>2</sup> Though these values are much lower than those present in rapid solidification processes (RSP), they represented solidification rates capable of achieving non-equilibrium cooling, from which amorphous or metastable-phase structures are easily realized.

The microstructure of the calcia–alumina IMS fibres affects fibre mechanical properties. Partial crystallization in 46.5 wt% CaO–53.5 wt%  $\text{Al}_2\text{O}_3$

IMS fibres has been shown to lead to as much as 97% increase in elastic modulus.<sup>2</sup> Though the crystalline phases responsible for this increase have not yet been identified, it is believed that the crystalline phase, estimated to be between 10 and 15% of the fibre, is present as nanocrystallites of a high-modulus compound, not unlike the more well-known lithium aluminosilicate glass-ceramics. The improvement in modulus is important for structural applications, particularly for Portland cement composites where calcia-alumina IMS fibres have been found to be chemically stable<sup>3</sup> and to improve composite compressive strengths.<sup>4</sup>

The calcia-alumina IMS fibres would be of even greater interest if their temperature resistance were better understood. Attempts have been made by three groups of researchers to elaborate upon crystallization processes in calcia-alumina IMS fibres. Wallenberger *et al.* heat treated IMS fibres of quarternary- and binary-oxide compositions at 1200°C for 1 h in alumina boats and found that all fibres crystallized completely.<sup>5</sup> XRD analysis of the fibres showed the presence of  $\text{CaAl}_2\text{O}_4$  in all samples and  $\text{Ca}_{12}\text{Al}_{14}\text{O}_{33}$  in two of the samples, including the only binary calcia-alumina fibre studied. DTA thermograms at 20°C min<sup>-1</sup> showed crystallization temperatures ranging from 969 to 1021°C in all amorphous fibres. No crystallization exotherms appeared in the subsequent heating cycles, indicating a fully-crystalline fibre. Sung *et al.* also performed DTA analyses on calcia-alumina IMS fibres and found that crystallization peaks ranged from 948 to 1034°C for the amorphous fibres over heating rates of 3–80°C min<sup>-1</sup>.<sup>6</sup> They were able to estimate the activation energy for crystallization at 477–490 kJ mol<sup>-1</sup>. Their XRD results of DTA samples showed the presence of  $\text{Ca}_{12}\text{Al}_{14}\text{O}_{33}$ , with  $\text{CaAl}_2\text{O}_4$  as a minor component. Finally, Mitchell *et al.* performed time-temperature crystallization studies on amorphous calcia-alumina IMS fibres at 900, 1000 and 1100°C for exposure times ranging from 6 to 6000 s.<sup>7</sup> These results indicated that crystallization can occur at temperatures as low as 900°C for exposure times approaching 6000 s, and that there is substantial liquid formation at 1100°C, well below the published eutectic melting point of the compound. XRD determinations of the crystallized fibres showed the presence of  $\text{Ca}_3\text{Al}_{10}\text{O}_{18}$  and  $\text{CaAl}_4\text{O}_7$ , as well as an unidentified, metastable phase at 900°C, and phases  $\text{Ca}_{12}\text{Al}_{14}\text{O}_{33}$ ,  $\text{CaAl}_4\text{O}_7$  and/or  $\text{Ca}_3\text{Al}_{10}\text{O}_{18}$ , at both 1000 and 1100°C.

The present investigation seeks to use DTA to elaborate upon both the crystalline transitions that occur in the amorphous filaments, and the cooling processes which can lead directly to crystalline

compounds from the melt. XRD data will then be used to connect the thermal history of the sample with phase identification.

## 2 EXPERIMENTAL

Filaments of a eutectic 46.5 wt%  $\text{CaO}$ –53.5 wt%  $\text{Al}_2\text{O}_3$  compound were produced in an inviscid melt spinning apparatus at the University of Wisconsin as described previously.<sup>8</sup> The resulting calcia-alumina fibres were approximately 380 microns in diameter, and had lengths of the order of 2–5 cm. A limited amount of archival fibre was available for analysis.

DTA was performed on ground fibre samples using an STA1500 + simultaneous, high-temperature differential scanning calorimeter (DSC)/thermogravimetric analyser (TGA) from Rheometric Scientific. After grinding, a 27.35 mg sample was placed in a platinum crucible. The reference pan was left empty to prevent any cross-contamination of the sample with  $\text{Al}_2\text{O}_3$ . Thermograms were collected over a temperature range of 600–1600°C in a nitrogen atmosphere for a heating-cooling-heating program. All programs were at a heating or cooling rate of 20°C min<sup>-1</sup>. After the final heating cycle, the heater was turned off and the sample allowed to cool at an undetermined rate.

The sample was then analysed for the presence of crystalline phases using XRD. DTA samples were re-ground, placed between quartz plates and placed in a Scintag XDS2000 X-ray diffractometer. Diffraction patterns were collected using a  $\text{Cu K}\alpha$  source ( $\lambda = 0.154 \text{ nm}$ ) with a Ni filter over a range of  $5^\circ < 2\theta < 60^\circ$ .

## 3 RESULTS AND DISCUSSION

The thermogram of the initial heating is shown in Fig. 1. The sloping baseline in all of the DTA scans to be presented can be attributed to unmatched thermal conductivities between the sample and (empty) reference pan. A slight change in heat capacity just below 900°C is clearly visible in Fig. 1. This second order transition would normally be attributed to a glass-transition, but may also be due to stress relaxation in the glassy fibre. The high IMS quench rates alluded to earlier not only “freeze in” amorphous structures, but also immobilize stress distributions that can only be relieved at elevated temperatures. Upon further heating, the sample in Fig. 1 exhibits the characteristic crystallization exotherm which peaks at 973°C, in good agreement with the results of Sung *et al.*<sup>6</sup> for

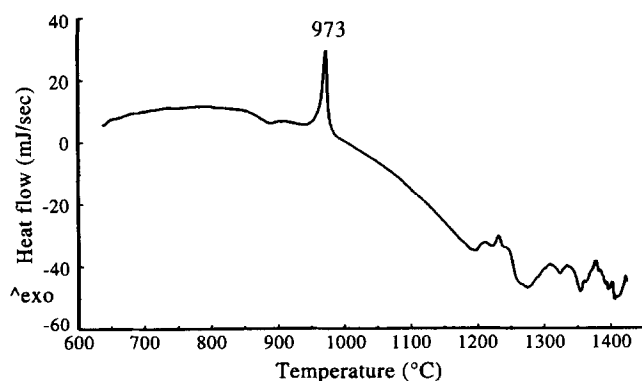


Fig. 1. Differential thermal analysis first heating curves at 20°C min<sup>-1</sup> in nitrogen for 46.5% CaO–53.5% Al<sub>2</sub>O<sub>3</sub> IMS ground fibres.

chopped fibre. Thus, it does not appear that grinding affects the amorphous–crystalline transition in these fibres at this heating rate.

Since Fig. 1 was obtained on a high-temperature, heat-flow design DTA, semi-quantitative information may be extracted from the crystallization peak. Integration of the peak in Fig. 1 gives a transition enthalpy of 8 J g<sup>-1</sup> (1.92 cal g<sup>-1</sup>), or 218 mJ for the entire sample. This energy is more characteristic of a displacive transformation, such as  $\alpha$ -SiO<sub>2</sub> to  $\beta$ -SiO<sub>2</sub> (10 J g<sup>-1</sup>)<sup>9</sup> rather than a reconstructive transformation such as crystallization. Nonetheless, previous X-ray diffraction studies have shown that these amorphous fibres are crystalline after this transition.<sup>2,6,7</sup> Broad exothermic events appear in Fig. 1 above 1200°C. It is difficult to assign these peaks to any specific transitions. TGA results (not shown) indicate that the overall weight loss is small in these fibre samples, and can be attributed entirely to buoyancy effects. A distinct melt endotherm is also not observed above 1200°C. This is highly unusual, since earlier results clearly show a melt endotherm not only in the first heating cycle, but the second as well.<sup>5</sup> However, those results were for a fibre of higher alumina content (67%), which may account for the sharper crystalline melting point of that fibre sample. The DTA results of Sung *et al.* are not helpful in this instance since their fibre samples were only heated to 1200°C,<sup>6</sup> well below the melting point of the eutectic compound.

Cooling curves have been neglected in previous studies, but constitute an important piece of information in the study of solidification phenomena in calcia–alumina IMS fibres. In previous studies where DTA has been performed on as-spun fibre samples to 1200°C, XRD results are representative of the phases present from crystallization during heat treatment. The next logical step is to perform DTA analysis after the sample has been heated above

the apparent melting point of the compound(s), after which point any crystalline phases present are due to solidification, and not from an amorphous–crystalline transition. Such a DTA cooling cycle for the fibre sample is shown in Fig. 2. This curve represents data collected between the first and second heating cycles, at a cooling rate of 20°C min<sup>-1</sup>. This figure shows a sharp, solidification exotherm at 1403°C followed by two smaller, exothermic events at 1242 and 1118°C, respectively. It is difficult to identify the compounds associated with these solidification exotherms based solely on published phase diagrams, which differ dramatically with regard to phase formation in and around the eutectic composition (near 50 wt% Al<sub>2</sub>O<sub>3</sub>). Three, two-phase regions can exist around the eutectic: Ca<sub>3</sub>Al<sub>2</sub>O<sub>6</sub> + liquid, CaAl<sub>2</sub>O<sub>4</sub> + liquid and Ca<sub>12</sub>Al<sub>14</sub>O<sub>33</sub> + liquid. Nurse *et al.*<sup>10</sup> have shown, however, that Ca<sub>12</sub>Al<sub>14</sub>O<sub>33</sub> can exist only in the presence of water, and that it has a melting point of 1392°C in air of normal humidity. According to these same authors, the “true” eutectic composition should melt congruently at 1360°C to form

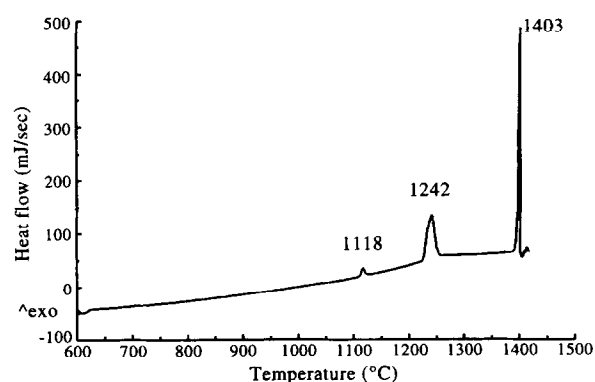


Fig. 2. Differential thermal analysis second heating curves at 20°C min<sup>-1</sup> in nitrogen for 46.5% CaO–53.5% Al<sub>2</sub>O<sub>3</sub> IMS ground fibres.

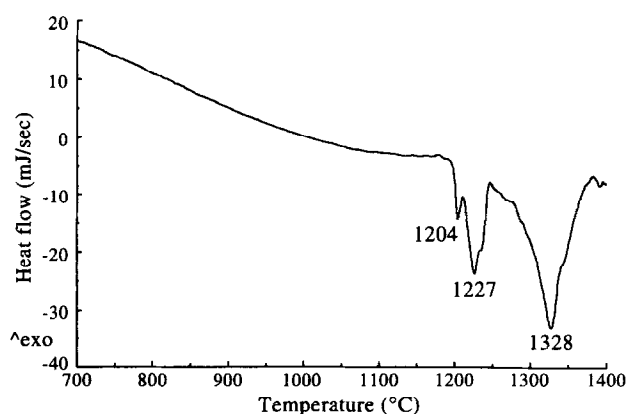


Fig. 3. Differential thermal analysis cooling curves at 20°C min<sup>-1</sup> in nitrogen for 46.5% CaO–53.5% Al<sub>2</sub>O<sub>3</sub> IMS ground fibres.

$\text{CaAl}_2\text{O}_4$  and  $\text{Ca}_3\text{Al}_2\text{O}_6$ . Hence, the melt exotherm upon cooling at  $1403^\circ\text{C}$  could be representative of solidification of either the eutectic compound or  $\text{Ca}_{12}\text{Al}_{14}\text{O}_{33}$ . Formation of a metastable phase (such as  $\text{Ca}_{12}\text{Al}_{14}\text{O}_{33}$ ) followed by transformation to equilibrium phases is also a possibility. This behaviour has been observed in amorphous calcia-alumina solids for  $\text{CaO} > 78.5\%$ .<sup>11</sup> In these studies, the author shows evidence for formation of a metastable,  $\gamma\text{-Al}_2\text{O}_3$ -type phase with Ca-ion defects, followed by transformation to a stable, monoclinic  $\text{CaAl}_2\text{O}_4$  structure. He estimates an activation energy of  $469\text{ kJ mol}^{-1}$  ( $112\text{ kcal mol}^{-1}$ ) for the metastable to monoclinic transition. The two, smaller exotherms at  $1232$  and  $1118^\circ\text{C}$  may be indicative of such transformations, or may be due to subeutectic liquid solidification. Visual evidence for liquid formation below the eutectic melting point comes from the heating studies of Mitchell *et al.*<sup>7</sup> It is possible that one or both of the solidification

exotherms at  $1242$  and  $1118^\circ\text{C}$  are due to small amounts of remnant liquid after the initial solidification at  $1403^\circ\text{C}$ .

Finally, the second heating cycle is shown in Fig. 3. The main item of interest here is the absence of crystallization transitions that were present in the first heating cycle. Thus, the fibre is highly crystalline during the second heating. The endotherm at  $1227^\circ\text{C}$  coincides with the exotherm at  $1242^\circ\text{C}$  observed in the cooling cycle. The strong endotherm at  $1328^\circ\text{C}$  may be that of the eutectic compound, but once again, a clear, melt endotherm near  $1400^\circ\text{C}$  is conspicuously absent from this trace.

An X-ray diffractogram for the sample after DTA experiments is shown in Fig. 4. The presence of  $\text{Ca}_3\text{Al}_2\text{O}_6$  and  $\text{CaAl}_2\text{O}_4$  is indicated. Average crystallite size, as determined from peak width, is estimated to be  $60\text{ nm}$ . The identified phases are consistent with published phase diagrams,<sup>9</sup> as described earlier. The compound  $\text{C}_{12}\text{Al}_{14}\text{O}_{33}$  was

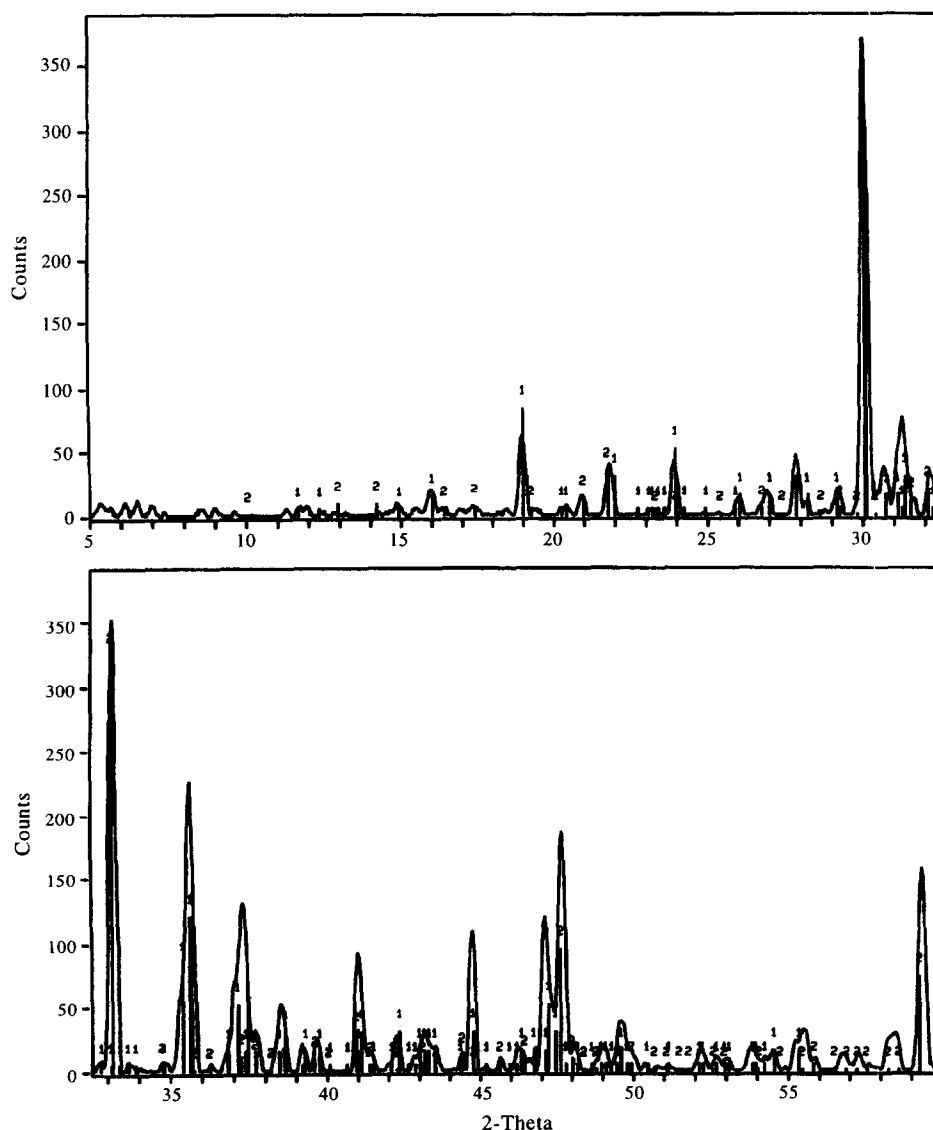


Fig. 4. X-ray powder diffractogram of 46.5%  $\text{CaO}$ –53.5%  $\text{Al}_2\text{O}_3$  IMS ground fibres after final cooling in DTA. Phases are labelled as follows: 1 =  $\text{CaAl}_2\text{O}_4$ ; 2 =  $\text{Ca}_3\text{Al}_2\text{O}_6$ .

absent, indicating anhydrous conditions. Though this particular compound has been identified in the majority of heat-treated calcia–alumina IMS<sup>7–5</sup> fibres, direct comparison of Fig. 4 with the literature XRD results is not possible, since the literature analyses were performed after heat treatment of amorphous fibres above the crystallization point, but below the eutectic melting point. This is a much different thermal history than cooling from the melt as performed here. Finally, since the final cooling rate was not regulated, direct comparison of the XRD results with the DTA cooling curve in Fig. 2 is not possible. Future investigations will incorporate XRD immediately after controlled cooling.

#### 4 CONCLUSIONS

DTA cooling curves have been used to show a solidification temperature of 1403°C in 46.5 wt% CaO–53.5 wt% Al<sub>2</sub>O<sub>3</sub> fibres, made by inviscid melt spinning (IMS), after heating to 1600°C. DTA heating curves indicate the presence of a crystalline transformation at 973°C upon heating of the amorphous fibres at 20°C min<sup>-1</sup>. Stress relaxation is also observed upon initial heating. Controlled cooling studies show a distinct solidification temperature of 1403°C, followed by smaller exothermic transitions, indicative of either sub-solidus liquid formation or transformation of a metastable phase. Subsequent heating cycles show no crystallization transformations, indicating near complete crystallization upon cooling between heating cycles. XRD results show that two different phases form during cooling from the melt, including CaAl<sub>2</sub>O<sub>4</sub> and Ca<sub>3</sub>Al<sub>2</sub>O<sub>6</sub>. For the first time, DTA cooling curves have been used to elaborate upon the solidification phenomena in the formation of calcia–alumina fibres by inviscid melt spinning. Although there is a large gap between the non-equilibrium quench rates of the IMS process and the controlled cooling rates of the DTA, further studies at higher quench rates will elaborate upon the sub-solidus liquid formation demonstrated here, and the mechanisms which ultimately lead to amorphous fibre formation.

#### ACKNOWLEDGEMENTS

The author wishes to thank Rheometric Scientific, Inc. for the DTA analyses. The help of Dr Stanley A. Dunn in the preparation of fibre samples and Mr Pierre Burnside of the Coordinated Instrumentation Facility at Tulane University for XRD analysis is gratefully acknowledged.

#### REFERENCES

1. CUNNINGHAM, R. E., RAKESTRAW, J. W. MOTTERN, W. J. PRIVOTT, L. F. & DUNN, S. A., Inviscid melt spinning of filaments via chemical jet stabilization. In *Spinning Wire from Molten Metals*, AICHe Symposium Series, Vol. 74, No. 180, ed. American Institute of Chemical Engineers, NY, 1978, p. 20.
2. DUNN, S. A. & PAQUETTE, E. G., Redrawn inviscid melt-spun fibres—potential low-cost composite reinforcement. *Adv. Ceram. Mater.*, **2**(4) (1987) 804.
3. YON, K. Y., MITCHELL, B. S., KOUTSKY, J. A. & DUNN, S. A., Chemical stability of inviscid melt-spun (IMS) fibres of calcia–alumina in aqueous media. *Mater. Chem. Phys.*, **34**(3–4) (1993) 219.
4. YON, K. Y., MITCHELL, B. S., KOUTSKY, J. A. & DUNN, S. A., Introduction of new reinforcement for cementitious materials—calcia–alumina (CA) fibres formed by the inviscid melt-spinning (IMS) process. *Cem. Conc. Compos.*, **15**(3) (1993) 165.
5. WALLENBERGER, F. T., WESTON, N. E. & DUNN, S. A., Inviscid melt spinning—IMS crystallization of amorphous alumina fibres. *SAMPE Q.*, **21**(3) (1990) 30.
6. SUNG, Y. M., DUNN, S. A. & KOUTSKY, J. A., Crystallization of inviscid melt spun (IMS) calcia–alumina eutectic fibres. *Ceram. Int.*, **21**(3) (1995) 169.
7. MITCHELL, B. S., YON, K. Y., KOUTSKY, J. A. & DUNN, S. A., Phase identification in calcia–alumina fibres crystallized from amorphous precursors. *J. Non-cryst. Solids*, **152** (1993) 143.
8. MITCHELL, B. S., Structure–property relationships in mixed metal oxide fibres formed via inviscid melt-spinning. Ph.D. thesis, Department of Chemical Engineering, University of Wisconsin-Madison, 1991.
9. SPEYER, R. F., *Thermal Analysis of Materials*. Dekker, NY, 1994, p. 63.
10. NURSE, R. W., WELCH, J. H. & MAJUMDAR, A. G., The CaO–Al<sub>2</sub>O<sub>3</sub> system in a moisture-free atmosphere. *Trans. Brit. Ceram. Soc.*, **64** (1965) 409.
11. VALLINO, M., Kinetic study of the crystallization of amorphous-derived CaO–2Al<sub>2</sub>O<sub>3</sub>, *Ceram. Int.*, **10**(1) (1984) 30.